

Surface roughening and scaling behavior of vacuum-deposited SnCl₂Pc organic thin films on different substrates

Sk. Md. Obaidulla and P. K. Giri

Citation: [Applied Physics Letters](#) **107**, 221910 (2015); doi: 10.1063/1.4936937

View online: <http://dx.doi.org/10.1063/1.4936937>

View Table of Contents: <http://scitation.aip.org/content/aip/journal/apl/107/22?ver=pdfcov>

Published by the [AIP Publishing](#)

Articles you may be interested in

[Effect of annealing on the growth dynamics of ZnPc LB thin film and its surface morphology](#)

[AIP Advances](#) **4**, 077126 (2014); 10.1063/1.4891177

[Functional properties of ZnO films prepared by thermal oxidation of metallic films](#)

[J. Appl. Phys.](#) **113**, 234506 (2013); 10.1063/1.4811357

[Radical modification of the wetting behavior of textiles coated with ZnO thin films and nanoparticles when changing the ambient pressure in the pulsed laser deposition process](#)

[J. Appl. Phys.](#) **110**, 064321 (2011); 10.1063/1.3639297

[Surface roughening evolution in pentacene thin film growth](#)

[Appl. Phys. Lett.](#) **98**, 243304 (2011); 10.1063/1.3599579

[Structural and electrical properties of metal contacts on n-type ZnO thin film deposited by vacuum coating technique](#)

[J. Vac. Sci. Technol. B](#) **27**, 2124 (2009); 10.1116/1.3196786

The image shows the cover of an Applied Physics Reviews journal issue. It features a blue and orange color scheme with a molecular structure background. The text 'NEW Special Topic Sections' is prominently displayed in white. Below it, 'NOW ONLINE' is written in yellow, followed by 'Lithium Niobate Properties and Applications: Reviews of Emerging Trends' in white. The AIP Applied Physics Reviews logo is in the bottom right corner.

NEW Special Topic Sections

NOW ONLINE
Lithium Niobate Properties and Applications:
Reviews of Emerging Trends

AIP Applied Physics Reviews

Surface roughening and scaling behavior of vacuum-deposited SnCl₂Pc organic thin films on different substrates

Sk. Md. Obaidulla¹ and P. K. Giri^{1,2,a)}

¹Department of Physics, Indian Institute of Technology Guwahati, Guwahati 781039, India

²Centre for Nanotechnology, Indian Institute of Technology Guwahati, Guwahati 781039, India

(Received 4 October 2015; accepted 20 November 2015; published online 3 December 2015)

The evolution of surface morphology and scaling behavior of tin (IV) phthalocyanine dichloride (SnCl₂Pc) thin films grown on Si(100) and glass substrates have been studied using atomic force microscopy (AFM) and height-height correlation function analysis. X-ray diffraction measurement confirms the crystalline nature of the SnCl₂Pc thin film on glass substrate, while no crystallographic ordering is present for the film grown on Si substrate. The growth exponent β is found to be much larger for the film on glass substrate (0.48 ± 0.07) as compared to that on Si substrate (0.21 ± 0.08), which may be due to the high step-edge barrier, so-called Ehrlich-Schwöbel barrier, resulting in the upward dominant growth on glass substrate. From the 2D fast Fourier transform of AFM images and derived scaling exponents, we conclude that the surface evolution follows a mound like growth. These results imply the superiority of glass substrate over the Si substrate for the growth of device quality SnCl₂Pc thin film. © 2015 AIP Publishing LLC. [<http://dx.doi.org/10.1063/1.4936937>]

Thin films based on molecular semiconductor, specifically “small” molecules like phthalocyanine are finding an increasing application in a number of optoelectronic devices. In particular, they have been exploited in organic light emitting diodes,¹ photovoltaic devices,^{2,3} and organic field-effect transistors, organic sensors⁴ due to their favorable properties, e.g., thermal and chemical stability, well ordered thin film growth and wide absorption band at the optical region. They also exhibit a certain degree of “specific tunability” due to various metals ion (M = Sn, Cu, CO, H₂, Zn, etc.) and the side groups (R = F, Cl, NH₂, O(CH₂)₁₀OH, etc.) that can be introduced within a broad range.⁵ The optimized transport phenomena like injection and recombination of charge carriers depend among other parameters, on molecular packing, range of grain boundaries/microstructure and roughness/morphology of surfaces. Therefore, the controlled deposition of molecular thin films is primarily a key requirement for the optimization of electro-optical properties in organic based devices in which the optimized film thickness with desired properties are essential. In this regard, the SnCl₂Pc is particularly attractive, since it is considered as a good candidate for n-type organic material and the device based on this molecule is relatively more stable.^{6,7} So, understanding the growth dynamics of organic thin films is one of the key issues in the field of organic electronics. In case of heterostructures, such as organic-organic heterostructures^{8,9} (for organic diode) and organic-inorganic heterostructures¹⁰ (for electrode/contacts), the knowledge of growth kinetics is of utmost importance, since their interfacial structures can play a crucial role on the scaling properties. However, there has been no report on the scaling behavior and growth dynamics of SnCl₂Pc on different substrates that are most relevant for device applications.

The scaling theory can be implemented to quantify the statistical properties of the surface morphology of thin films and to formulate theoretical models of growth modes for different inorganic materials such as metals,^{11,12} semiconductors,^{13,14} organic like polymers,¹⁵ and small molecules.^{16,17} In this work, we elucidate the change of surface morphology of SnCl₂Pc with thickness variation, and we address the effect of substrate-surface on the roughness scaling behavior. From the height–height correlation function (HHCF) and theoretical formalism of scaling theory, we have calculated the growth exponents, and these exponents describe the morphological features of SnCl₂Pc thin films.

SnCl₂Pc (n-type) thin films were grown in a high vacuum organic thermal evaporation chamber with a base pressure of $\sim 10^{-6}$ mbar. Commercially available SnCl₂Pc (Alfa Aesar, 97%) molecules sublimed from self-assembled effusion cell were deposited onto well cleaned Si(100) and glass substrates at room temperature under identical conditions. The substrates were first cleaned separately by deionized water (18.2 M Ω cm), acetone, and 2-propanol with sonication for 15 min each. The cleaned substrates were preheated to $>300^\circ\text{C}$ and subsequently cooled slowly to room temperature. During the vacuum deposition, the cell temperature was maintained at $\sim 350 \pm 2^\circ\text{C}$, and molecules were condensed on the Si and glass substrates. The average growth rate ($\sim 0.2\text{--}0.3 \text{ \AA/s}$) of the film was optimized by a thickness monitor during the growth. SnCl₂Pc thin films with different thicknesses (8–87 nm) were deposited for different times and characterized *ex situ* by atomic force microscopy (AFM) (Agilent-5500), high power X-ray diffractometer (XRD) (Rigaku), X-ray photoelectron spectroscopy (XPS) (ULVAC-PHI), and UV-Visible spectroscopy (UV-Vis) (JASCO, V-630). Thermogravimetric analysis (TGA) (NETZSCH) was carried out in Ar gas up to 1000°C .

TGA shows that the SnCl₂Pc molecules are stable up to a temperature of 450°C .¹⁸ As the sublimed temperature here is $\sim 350^\circ\text{C}$, the molecules are not fragmented during the deposition on various substrates. The surface morphology was

^{a)}Author to whom correspondence should be addressed. Electronic mail: giri@iitg.ernet.in.

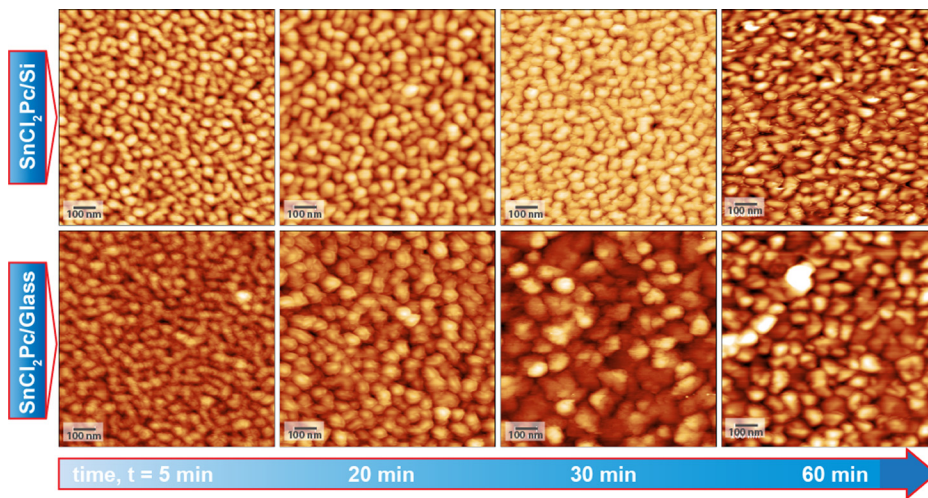


FIG. 1. Representative AFM topography images (scan size: $1\ \mu\text{m} \times 1\ \mu\text{m}$) of SnCl_2Pc thin films for different deposition times 5, 20, 30, and 60 min on Si(100) substrate (top panel) and glass substrate (bottom panel) (thickness 8, 35, 51, and 87 nm, respectively).

analyzed by AFM measurements in the tapping mode (size: 512×512 pixel) to avoid any damage to the film. Repeated measurements were carried out at different locations of a sample in order to ensure that no changes occurred due to tip-sample interaction. Representative AFM images ($1\ \mu\text{m} \times 1\ \mu\text{m}$) taken at various stages of the growth of SnCl_2Pc thin film are shown in Fig. 1. The upper panel shows the morphology for SnCl_2Pc thin film grown on Si substrate, while the lower one shows that on glass substrate for growth time $t = 5, 20, 30,$ and 60 min. Initially, SnCl_2Pc forms nearly spherical grains on both Si as well as glass substrates. The surface features enlarge with increasing growth time. As the thickness of SnCl_2Pc films increases, the grains are nucleated on the both substrates similar to other phthalocyanine based thin films. At higher thickness, the average grain size (~ 15 nm) is bigger for SnCl_2Pc film on glass as compared to that on Si substrate (~ 9 nm), as measured from the AFM images.¹⁸ The nearly spherical shape of the islands (spherical crystallites) indicates negligible anisotropy, which is a characteristic morphology for phthalocyanine derivatives.¹⁹

In order to understand the dynamic scaling behavior and to gain a detailed insight into the growth processes, we have calculated the scaling exponents and root mean square (RMS) local slope of the mounds. These quantities can be obtained by calculating the HHCF, $g(r, t)$, which is defined as the mean square of height difference between two surface positions separated by a lateral distance r ($=\sqrt{(x-x')^2 + (y-y')^2}$). If scaling exists, it is of the form,^{20,21} $g(r, t) = \langle [h(r+r', t) - h(r', t)]^2 \rangle = 2w(t)^2 g\left(\frac{r}{\xi(t)}\right)$, where spatial averaging is done over r' variable of the planar sample surface. HHCF can be evaluated from real space images by spatial averaging over one or several regions, which should be much larger than r to avoid edge effects. The relative magnitudes of r and the correlation length ξ (beyond which surface heights are uncorrelated on the average) can divide the HHCF into two distinct behaviors: (i) $r \ll \xi$, $g(r) \propto r^{2\alpha}$, where α ($0 \leq \alpha \leq 1$) is the roughness scaling exponent, which describes the surface fractality, and (ii) $r \gg \xi$, $g(r) = 2w^2$, where $w = \langle (h - \langle h \rangle)^2 \rangle^{1/2}$ is the standard deviation of the surface height/RMS roughness. The parameters ξ and w are dependent on the deposition time, t ,

and follow the power laws as $w \propto t^\beta$ and $\xi \propto t^{1/z}$, where β and $1/z$ are growth and dynamic scaling exponents, respectively, and in many systems, they are related to $1/z \cong \beta/\alpha$.^{11,12} The ξ , which at each thickness is determined by fitting the HHCF, where the two regimes $r \ll \xi$ and $r \gg \xi$ are connected to a function for self-affine surface, which manifest anisotropic scale invariance,²² is given by

$$g(r) = 2w^2 \left[1 - \exp \left\{ - \left(\frac{r}{\xi} \right)^{2\alpha} \right\} \right]. \quad (1)$$

For self-affine surface, the roughness scaling follows a simple power law with a growth exponent β and roughness exponent α , which unambiguously distinguish the growth universality classes.

From Fig. 2(a), it is perceptible that HHCF $g(r, t)$ increases linearly with r at small r and saturates at large r , with the asymptotic behavior predicted by Eq. (1). The lateral positions corresponding to a grain yields ξ , which is a measure of the average island size. It is clear from Figs. 2(a) and 3(a) that $g(r, t)$ shifts upward as growth time progresses or SnCl_2Pc film thickness increases, which is consistent

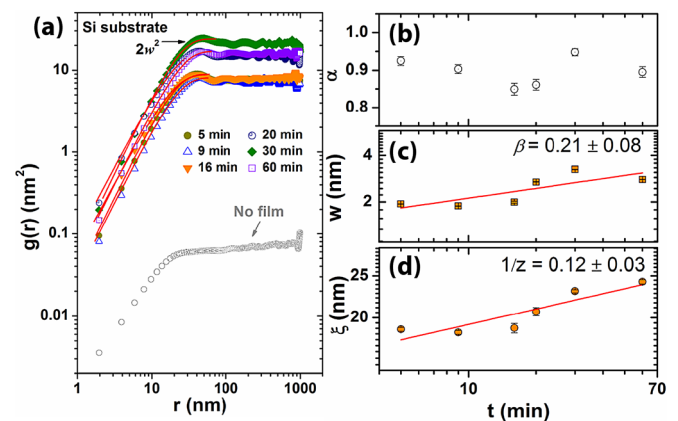


FIG. 2. (a) HHCF $g(r)$ as a function of distance r with best fitted theoretical curve for SnCl_2Pc thin films on Si substrate with different deposition times. The symbols are experimental data and the solid lines are fit to Eq. (1). (b) α , (c) w , and (d) ξ as a function of deposition time, t .

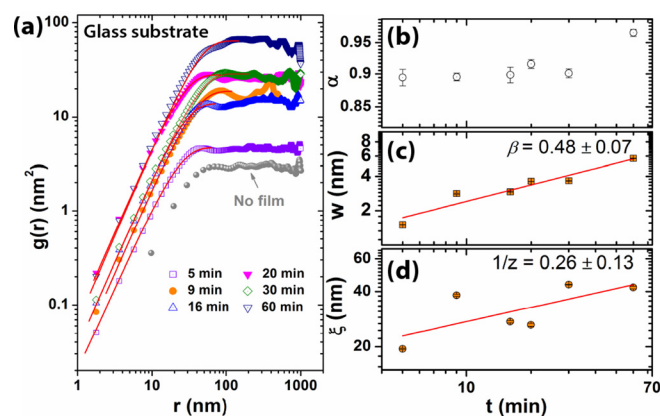


FIG. 3. (a) HHCF $g(r)$ vs. distance r with best fitted theoretical curve (solid line) for SnCl₂Pc thin films on glass substrate with different deposition times. (b) α , (c) w , and (d) ξ as a function of deposition time, t .

with the results of other organic thin films.^{16,19} From HHCF function analysis, the calculated average roughness exponent, α is ~ 0.90 for both Si and glass substrates [see Figs. 2(b) and 3(b)].

Next, we measured the growth exponent β ($w \propto t^\beta$) of the SnCl₂Pc films. At the initial stage of growth, β is nonzero for both cases. From Fig. 2(b), we measured $\beta = 0.21 \pm 0.08$ and 0.48 ± 0.07 for SnCl₂Pc on Si and glass, respectively. Thus, a large β value (0.48 ± 0.07) is observed for the growth on glass substrate in contrast to the small β value observed for Si substrate. The large β value of SnCl₂Pc on glass substrate suggests that the growth front is roughening and it implies a large step-edge barrier or Ehrlich-Schwöbel (ES) barrier that does not allow atoms to diffuse over the edge of step on the surface, resulting in the uphill current of diffusive particle,²³ and different plane of stacking directions between the domains, which comes from the intrinsic anisotropy of the molecular structures and their crystallographic ordering. The influence of deep grain boundaries on the growth exponent has been described using (1 + 1)-dimensional surface growth-model by Yim and Jones,¹⁶ and this may contribute to the high β value due to tilted upward orientation of slip-stacked SnCl₂Pc molecules on the glass substrate. High β value (>0.5) is common to growth situations where unusually rapid roughening takes place, as expected for random deposition in “hit-and-stick” model, which could arise from non-local effects, such as shadowing effect or bulk diffusion.^{21,24–26} The anomalous large $\beta > 0.5$ values have been reported for several organic-molecular crystalline thin film systems, e.g., free-base H₂Pc on glass ($\beta = 1.02 \pm 0.08$),²⁷ ZnPc on glass ($\beta = 0.62 \pm 0.04$),¹⁹ diindeno perylene on SiO₂ ($\beta = 0.75$),²⁸ and F₁₆CuPc on ITO coated glass ($\beta \sim 3.089$).²⁹ These values are higher than those predicted by the random deposition model.²¹ On the other hand, small β value for Si substrate may be attributed to small ES barrier at edge of the molecular layer. A decrease in the crystallographic ordering of the films may be due to reduced step-edge barrier, although several studies have reported significant differences in the β values obtained for amorphous and crystalline films.³⁰ It is believed that phthalocyanines tend to grow in a standing-up configuration in thicker film on chemically “inert” glass substrate as compared to single

crystalline Si substrate. This different growth modes observed on two different substrates can be understood in terms of molecule-substrate interactions, since molecule-molecule interaction strength is nearly the same for all investigated films. Here, the molecule-substrate interaction strength may be stronger for Si substrate than the glass substrate. So, the adsorption of the molecule occurs in a lying geometry of SnCl₂Pc molecules on Si substrate.³¹ Our XPS analysis on 5 nm thin SnCl₂Pc film on Si and glass substrate shows different oxygen concentrations in the film and the Si 2p spectrum of the Si substrate shows Si⁴⁺, Si³⁺, and Si²⁺ oxidation states corresponding to different suboxides of Si, which are due to the native oxides.¹⁸ Thus, the nature of molecular interactions in two different substrates are likely to be different, giving rise to different molecular structures. We find the dynamic scaling exponents $1/z \sim 0.12 \pm 0.03$ and 0.26 ± 0.13 for SnCl₂Pc thin films on Si and glass substrate, respectively (see Figs. 2(d) and 3(d)). This indicates that the molecules grow in an upward direction rather than lateral direction on glass substrate and higher density of grains is formed on glass than Si within the same scan area ($1 \mu\text{m} \times 1 \mu\text{m}$). Thus, during the growth, the SnCl₂Pc molecule, which is intrinsically anisotropic, can change its orientation due to its orientational degrees of freedom (standing-up or lying-down). The anisotropic interactions with the surface of the substrates (inert or reactive) may play a significant role upon the scaling relations predicted by growth dynamic theories. This information would be important to understand the growth mechanism of molecular thin films and to control the interfacial properties of the films.³²

Interestingly, the calculated exponents (α , β , $1/z$) are quite close to the exponents predicted by the model of mound formation,⁸ which is reported for both organic and inorganic materials. Although the asymptotic value of roughness exponent $\alpha = 1$ for mound formation, in practice, a lower value can be obtained.¹⁴ We have plotted 2D fast Fourier transform (FFT) of the surfaces from the representative AFM images on Si and glass substrates, as shown in Figs. 4(a) and 4(b), respectively. It clearly shows a ring like behavior, which supports the mound growth morphology.^{8,33} Further, the HHCF is oscillatory in nature for mounded surfaces, which is clearly visible at large r from Figs. 2(a) and 3(a). The formation of mound on surface can be attributed to different growth effects

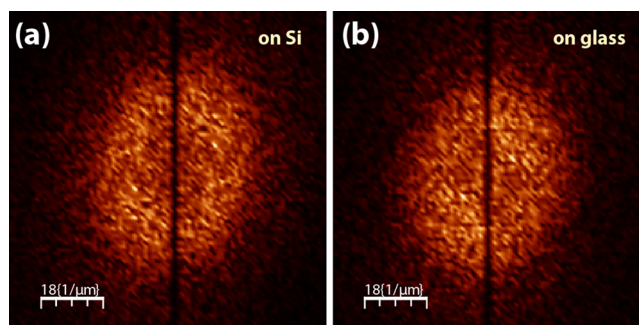


FIG. 4. 2D FFT pattern of the AFM images of SnCl₂Pc thin film of thickness ~ 8 nm (deposited for 5 min) on: (a) Si and (b) glass substrate. The vertical dark line in the center of each image is due to the AFM fast scan direction.

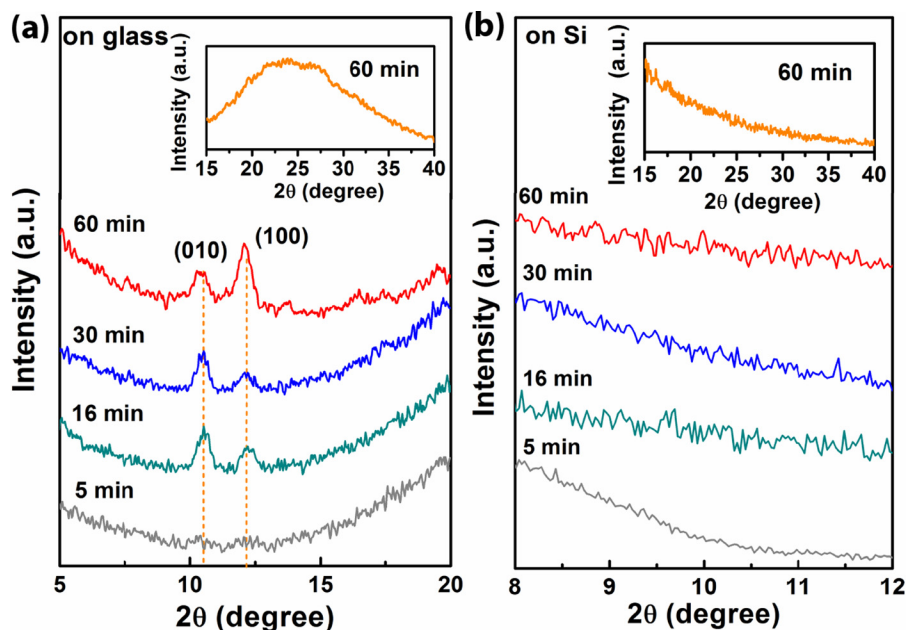


FIG. 5. XRD patterns of SnCl_2Pc thin films grown on (a) glass, and (b) Si substrate for different deposition times (5–60 min). The inset shows the XRD pattern for thick film (60 min) in the extended range $15^\circ\text{--}40^\circ$ for glass and Si substrates.

such as step-edge barrier, diffusion effect, shadowing, and re-emission, and the mound formation may be local or non-local in nature.^{33,34}

The structural quality of the SnCl_2Pc films has been evaluated from XRD measurements. Figures 5(a) and 5(b) show the XRD pattern of SnCl_2Pc thin films grown on glass and Si substrates, respectively. For the films on glass (Fig. 5(a)), peaks at $2\theta \sim 10^\circ$ and $\sim 12^\circ$ are prominent for film thickness above ~ 8 nm. The inset shows the XRD pattern in the extended range of $2\theta = 15^\circ\text{--}40^\circ$ in each case. The film on the glass substrate shows a broad peak centered at $\sim 25^\circ$ arising from the glass substrate, while no such peak was observed for the case of Si substrate. The SnCl_2Pc thin film deposited on glass substrate is identified as triclinic crystallites ($a = 0.7363$ nm, $b = 0.8676$ nm, and $c = 1.1048$ nm, $\alpha = 74.21^\circ$, $\beta = 80.33^\circ$, and $\gamma = 85.47^\circ$),³⁵ while the film on Si substrate appears amorphous like, as evidenced by the absence of any diffraction peak even for ~ 87 nm thick film (see Fig. 5(b)).¹⁸ The peaks corresponding to inter-planar spacing $d_{(010)}$ and $d_{(100)}$ of 8.46 Å, and 7.29 Å are due to the diffraction from the (010) and (100) planes of the SnCl_2Pc crystallites, and it is due to the two different kinds of slip-stacked molecular packing formed on the glass substrate, which implies that the intermolecular $\pi\text{-}\pi$ direction is parallel to the glass substrate and it is useful for optoelectronic devices.^{6,36} In contrast, for SnCl_2Pc films on Si (see Fig. 5(b)), no predominant peak was observed for the range of the thicknesses (8–87 nm) studied here, even at different grazing angles of XRD¹⁸ and it reveals the amorphous nature of the SnCl_2Pc film. A possible reason for lying-down molecular geometry of SnCl_2Pc without any ordered arrangement is its tetragonal-bipyramidal (non-planar disk like) structure, and it would prevent it from crystallizing on the Si substrate with diamond structure. The amorphous characteristic of SnCl_2Pc thin films on Si may be due to very small extra energy required at the step edge when the molecules move down to the lower layer. The small β value of SnCl_2Pc film on Si can be rationalized by the small step-edge barrier and amorphous nature of the film. Note that no XRD peak was observed for

the SnCl_2Pc films of thickness below 8 nm on both the substrates. Although the intensity of the XRD pattern is dependent on film thickness, there is no significant shift in the Q-band peak position in the UV-Vis spectra for different samples,¹⁸ consistent with earlier reports.³⁷

Further, it is found that the height distribution $p(h)$ function is skewed negatively on Si and positively on glass substrate,¹⁸ where the skewness $S (= \frac{\langle (h-\langle h \rangle)^3 \rangle}{\sigma^3})$ is compared with a Gaussian distribution, which indicates the violation of the $h \rightarrow -h$ symmetry and thus the presence of a nonlinearity $((\nabla h)^2)$ associated with growth dependence on the local surface inclination.³⁸ However, the calculated exponents do not match with the reported Kardar-Parisi-Zhang (KPZ) growth model, $\frac{\partial h}{\partial t} = v\nabla^2 h + b(\nabla h)^2 + \eta$, where $v\nabla^2 h$ appears due to surface relaxation and η represents random Gaussian during deposition.^{39,40} Interestingly, the scaling exponents (α , β , and $1/z$) of organic SnCl_2Pc thin films is not consistent with any of the universality classes described by the conserved growth equations for kinetic growth developed for inorganic materials. Note that the β value for SnCl_2Pc on Si is quite comparable with that of F_{16}CuPc on ITO coated glass.⁴¹

In conclusion, we addressed the structural evolution of SnCl_2Pc thin films grown by thermal evaporation on Si and glass substrates. The growth dynamics of SnCl_2Pc thin films has been studied using AFM and HHCF analysis. Analyzing the scaling behavior and 2D fast Fourier transforms, it is concluded that the morphological evolution of the deposited SnCl_2Pc molecules follows mound like formation, which suggests that the SnCl_2Pc crystallites grow in the upward direction as the film thickness increases on glass substrate, which may be due to the high potential barrier or step-edge barrier. One of the important findings is that the β value for SnCl_2Pc thin film on glass substrate is comparable to that predicted by the random deposition model, while for Si substrate it is very small and results in “smoothing”—a lying down geometry, which may be due to the small step-edge barrier. SnCl_2Pc films grown here on glass substrate exhibited crystalline behavior, which is suitable for device fabrication.

The authors thank Central Instruments Facility (CIF) for AFM, TGA and DST-FIST, Government of India, for providing XRD facility. We acknowledge the financial support from CSIR (Grant No. 03(1270)/13/EMR-II), DEITY (Grant No. 5(9)/2012-NANO), and BRNS (Grant No. 2012/37P/1/BRNS). We thank Dr. K. Imakita, Kobe University, and Mr. R. Ghosh for help in the XPS analysis. We thank Professor Y. N. Mohapatra and Mr. Subhash Singh, IIT Kanpur for help in the XRD measurement.

- ¹T. C. Rosenow, K. Walzer, and K. Leo, *J. Appl. Phys.* **103**, 043105 (2008).
- ²F. Yang, M. Shtein, and S. R. Forrest, *Nat. Mater.* **4**, 37 (2005).
- ³T. Zhuang, Z. Su, Y. Liu, B. Chu, W. Li, J. Wang, F. Jin, X. Yan, B. Zhao, F. Zhang, and D. Fan, *Appl. Phys. Lett.* **100**, 243902 (2012).
- ⁴F. I. Bohrer, C. N. Colesniuc, J. Park, M. E. Ruidiaz, I. K. Schuller, A. C. Kummel, and W. C. Trogler, *J. Am. Chem. Soc.* **131**, 478 (2009).
- ⁵Z. Bao and J. Locklin, *Organic Field-Effect Transistors* (CRC Press, Boca Raton, FL, USA, 2007).
- ⁶D. Song, H. Wang, F. Zhu, J. Yang, H. Tian, Y. Geng, and D. Yan, *Adv. Mater.* **20**, 2142 (2008).
- ⁷S. Md. Obaidulla, D. K. Goswami, and P. K. Giri, *Appl. Phys. Lett.* **104**, 213302 (2014).
- ⁸Y. Zhang, E. Barrena, X. Zhang, A. Turak, F. Maye, and H. Dosch, *J. Phys. Chem. C* **114**, 13752 (2010).
- ⁹D. Hong, Y. R. Do, H. T. Kwak, and S. Yim, *J. Appl. Phys.* **109**, 063507 (2011).
- ¹⁰S. Zorba, L. Yan, N. J. Watkins, and Y. Gao, *Appl. Phys. Lett.* **81**, 5195 (2002).
- ¹¹J. H. Jeffries, J. K. Zuo, and M. M. Craig, *Phys. Rev. Lett.* **76**, 4931 (1996).
- ¹²G. Palasantzas and J. Krim, *Phys. Rev. Lett.* **73**, 3564 (1994).
- ¹³M. Pelliccione, T. Karabacak, C. Gaire, G. C. Wang, and T. M. Lu, *Phys. Rev. B* **74**, 125420 (2006).
- ¹⁴G. Lengel, R. J. Phaneuf, E. D. Williams, S. Das Sarma, W. Beard, and F. G. Johnson, *Phys. Rev. B* **60**, R8469 (1999).
- ¹⁵Y. P. Zhao, J. B. Fortin, G. Bonvallet, G. C. Wang, and T. M. Lu, *Phys. Rev. Lett.* **85**, 3229 (2000).
- ¹⁶S. Yim and T. S. Jones, *Appl. Phys. Lett.* **94**, 021911 (2009).
- ¹⁷S. Zorba, Y. Shapir, and Y. Gao, *Phys. Rev. B* **74**, 245410 (2006).
- ¹⁸See supplementary material at <http://dx.doi.org/10.1063/1.4936937> for TGA plot and molecular structure, AFM images with height profile XPS analysis, XRD pattern, UV-Vis absorption spectra, and height distribution function plot.
- ¹⁹J. Kim, N. Lim, C. R. Park, and S. Yim, *Surf. Sci.* **604**, 1143 (2010).
- ²⁰F. Family and T. Vicsek, *Dynamics of Fractal Surfaces* (World Scientific, Singapore, 1991).
- ²¹A. L. Barabási and H. E. Stanley, *Fractal Concepts in Surface Growth* (Cambridge University Press, Cambridge, 1995).
- ²²S. K. Sinha, E. B. Sirota, S. Garoff, and H. B. Stanley, *Phys. Rev. B* **38**, 2297 (1988).
- ²³S. Yim, K. I. Kim, and T. S. Jones, *J. Phys. Chem. C* **111**, 10993 (2007).
- ²⁴G. Zhang, B. L. Weeks, and M. Holtz, *Surf. Sci.* **605**, 463 (2011).
- ²⁵S. Kowarik, A. Gerlach, and F. Schreiber, *J. Phys.: Condens. Matter* **20**, 184005 (2008).
- ²⁶L. Vázquez, J. M. Albella, R. C. Salvarezza, A. J. Arvia, R. A. Levy, and D. Perese, *Appl. Phys. Lett.* **68**, 1285 (1996).
- ²⁷S. Yim and T. S. Jones, *Phys. Rev. B* **73**, 161305 (2006).
- ²⁸A. C. Dürr, F. Schreiber, K. A. Ritley, V. Kruppa, J. Krug, H. Dosch, and B. Struth, *Phys. Rev. Lett.* **90**, 016104 (2003).
- ²⁹J. L. Yang, S. Schumann, and T. S. Jones, *J. Phys. Chem. C* **114**, 1057 (2010).
- ³⁰S. Kowarik, A. Gerlach, S. Sellner, F. Schreiber, J. Pflaum, L. Cavalcanti, and O. Kononov, *Phys. Chem. Chem. Phys.* **8**, 1834 (2006).
- ³¹H. Peisert, T. Schwieger, J. M. Auerhammer, M. Knupfer, M. S. Golden, J. Fink, P. R. Bressler, and M. Mast, *J. Appl. Phys.* **90**, 466 (2001).
- ³²F. Schreiber, *Phys. Status Solidi A* **201**, 1037 (2004).
- ³³Y. Zhao, G.-C. Wang, and T.-M. Lu, *Characterization of Amorphous and Crystalline Rough Surface: Principles and Applications* (Academic Press, New York, 2001), Vol. 37.
- ³⁴G. Hlawacek, P. Puschnig, P. Frank, A. Winkler, C. Ambrosch-Draxl, and C. Teichert, *Science* **321**, 108 (2008).
- ³⁵J. Janczak and R. Kubiak, *Acta Crystallogr., Sect. C* **59**, m237 (2003).
- ³⁶S. M. Obaidulla and P. K. Giri, *J. Mater. Chem. C* **3**, 7118 (2015).
- ³⁷M. M. El-Nahass, K. F. Abd-El-Rahman, A. A. Al-Ghamdi, and A. M. Asiri, *Phys. B* **344**, 398 (2004).
- ³⁸J. T. Drotar, Y. P. Zhao, T. M. Lu, and G. C. Wang, *Phys. Rev. E* **59**, 177 (1999).
- ³⁹D. Tsamouras, G. Palasantzas, and J. T. M. De Hosson, *Appl. Phys. Lett.* **79**, 1801 (2001).
- ⁴⁰B. M. Forrest and L.-H. Tang, *Phys. Rev. Lett.* **64**, 1405 (1990).
- ⁴¹J. Yang, S. Yim, and T. S. Jones, *Sci. Rep.* **5**, 9441 (2015).